I&EC research
Industrial & Engineering Chemistry Research

Article

pubs.acs.org/IECR

Optimization of Experimental Parameters to Suppress Nozzle Clogging in Inkjet Printing

Ayoung Lee,[†,§] Kai Sudau,[‡] Kyung Hyun Ahn,[†] Seung Jong Lee,[†] and Norbert Willenbacher*[,§]

[†]School of Chemical and Biological Engineering, Institute of Chemical Process, Seoul National University, Seoul 151-744, Korea

[‡]InnovationLab GmbH, Speyerer Straße 4, 69115 Heidelberg, Germany

[§]Institute of Mechanical Process Engineering and Mechanics, Karlsruhe Institute of Technology, Gotthard-Franz-Straße 3, 76131 Karlsruhe, Germany

ABSTRACT: Stable drop jettability is mandatory for a successful, technical scale inkjet printing, and accordingly, this aspect has attracted much attention in fundamental and applied research. Previous studies were mainly focused on Newtonian fluids or polymer solutions. Here, we have investigated the drop jetting for zinc oxide (ZnO) particulate suspensions. Generally, the inverse Ohnesorge number $Z = Oh^{-1}$, which relates viscous forces to inertia and surface tension, is sufficient to predict the jettability of single phase fluids. For the inkjet printer setup used here, jetting was possible for Newtonian fluids with $2.5 < Z < 26$, but in the identical Z-range, nonjetting and nozzle clogging occurred for certain suspensions. A so-called ring-slit device, which allows for simultaneous formation and detection of aggregates in strongly converging flow fields, and single particle detecting techniques, which allow for an accurate determination of the number and size of micrometer-sized aggregates in suspensions of nanoparticles, were used to study this phenomenon. Nozzle clogging is induced by heterocoagulation of micrometer-sized aggregates and ZnO nanoparticles in the elongational flow field at the nozzle exit. Clogging may occur even if the size of these aggregates is well below the nozzle diameter and their concentration is on the order of only a few hundred parts per million (ppm). Accordingly, increased colloidal stability of nanoparticles and reduced aggregate concentration result in better drop jettability. Also, a nozzle design resulting in a shorter exposure time of the ink to elongational flow and an increased flow velocity helps to avoid nozzle clogging.

INTRODUCTION

Inkjet printing is an important direct patterning process for micro/nanofabrications of components such as polymer electronics,[1−3] field effect transistor (FET),[4−10] or solar cells.[11] For a successful patterning, the ink formulation should be well designed not only for drop jettability and uniform deposition but also for electrical performance of the printed structure after drying. As for drop jettability, the dynamics of a colloidal suspension jet is known to be different from that of a Newtonian liquid in terms of nonstraight flying trajectories and nonaxisymmetric ligaments.[12] The poor jetting behavior brings out difficulties and irregularities in the printing process. In spreading and leveling,[13,14] Marangoni flow, which is caused by concentration gradient and particle adsorption to the liquid−air interface, and non-Newtonian flow behavior influence the leveling process and may sometimes cause the so-called coffee ring effect. Drying conditions and especially the time scale of drying control the microstructure of the printed film, in particular its porosity and particle ordering.[15] Nevertheless, due to the complexities not only of the printing process, which include both shear and strong elongational flow fields at high fluid velocities, but also of the ink composition itself, characterizing and analyzing the jetting phenomena under strong flow fields are very important and challenging.

Many factors affect the performance of drop-on-demand inkjet printing. They include processing parameters[16−18] such as driving voltage (pulse height), dwell time (pulse width), and repetition rate, as well as fluid properties[19−21] such as surface tension σ, viscosity η, and density ρ. For Newtonian fluids, drop formation is determined by the dimensionless number, $Z = (d\rho\sigma)^{1/2}/\eta$, where d is the nozzle diameter, which is the characteristic length scale of the printing head. Z is often called inverse Ohnesorge number Oh^{-1} and is related to the Reynolds (Re) and Weber (We) numbers, $Z = Oh^{-1} = Re/We^{1/2}$. If Z is too low, no droplet can be formed, and if Z is too high, the formation of satellite droplets results in poor printing quality. Tai et al.[22] observed drop ejection in the range of $0.67 < Z < 50$ for aqueous mixtures of varying glycerol compositions (0−80 wt %) with nozzle diameter $d = 50$ μm.

The printing quality can be improved by adding a small amount of a high molecular weight polymer. It means that even when two inks are in similar range of Z the jettability can be changed by polymer addition suppressing the formation of satellite droplets. To reflect the feature of this kind, additional rheological parameters need to be considered. For polymer solutions, the complex shear modulus $G^* = G' + iG''$ or the extensional viscosity may be used, and since inkjet printing is a fast process the storage and loss moduli, G' and G'' at high frequency may be most relevant.[22−25]

For particulate inks including metallic or semiconducting nanoparticles, dispersion stability should be controlled since small particles tend to aggregate, which eventually affects printing quality. Surfactants or polymeric additives adsorbing

Received: May 29, 2012
Revised: August 31, 2012
Accepted: September 6, 2012
Published: September 6, 2012

dx.doi.org/10.1021/ie301403g | *Ind. Eng. Chem. Res.* 2012, 51, 13195−13204

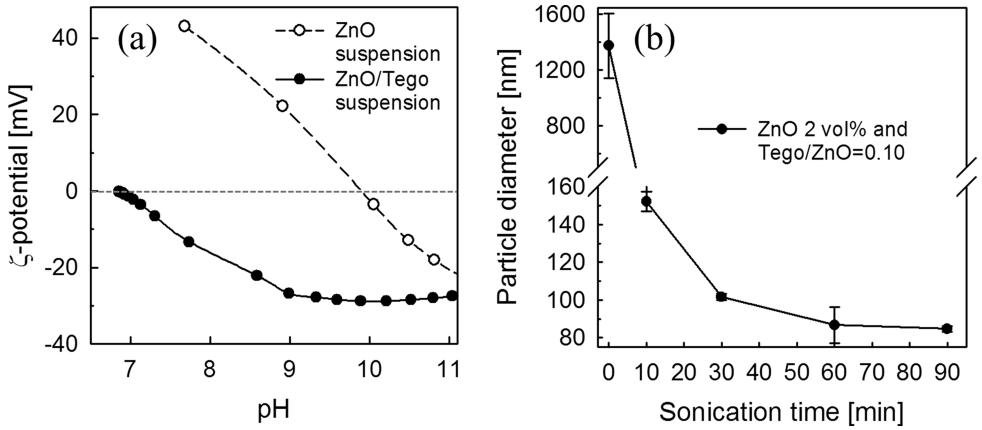

Figure 1. (a) ζ-potential as a function of pH for neat and polymer stabilized ZnO dispersions. (b) Mean particle size by dynamic light scattering for suspensions with 2 vol % ZnO and Tego/ZnO (w/w) = 0.10, and horn-type ultrasonication was conducted as a function of time (at a power of 32 W). The suspension was diluted to 1/300 of the initial concentration to meet the detectable range of the apparatus.

on the particle surface are often used to prevent aggregation or agglomeration but may disturb the electronic performance of the final printed product. Thus, the key for ink preparation is to satisfy both dispersion stability and electrical performance.

On the other hand, even if an extended shelf life and manufacturing stability of the suspensions is satisfied, instability may occur in the strong flow in the printing head and may lead to misfiring or even nozzle clogging. In other words, nonjetting can take place even if Z is in the appropriate jettable range; thus, Z alone is incapable of characterizing drop formation. Reis et al.[26] have suggested the drop jettable range for concentrated alumina wax suspensions as $1 < Z < 10$. However, the flow behavior inside the nozzle has been paid less attention.

The clogging during the flow through narrow channels is an extremely complex phenomenon. Such clogging can be caused by a small fraction of aggregates or impurities present in the ink, which are larger than the nozzle diameter (size exclusion). It can be also due to shear-induced gelation in liquid-like colloidal systems[27−29] or hydrodynamic bridging,[30] which may occur when several particles arrive at the nozzle entrance simultaneously and make particle bridges, even if these particles are an order of magnitude smaller than the nozzle diameter. This effect is more pronounced when the flow rate is higher. Furthermore, clogging can also occur due to fouling,[31] that is, particle deposition at the nozzle wall, and then, it is influenced by the choice of the nozzle material.

Recently, it has been shown that heterocoagulation of nanoparticles with micrometer-sized particles can also lead to flow-induced aggregation and clogging in the microchannels. This phenomenon may occur even if the fraction of large particles is on the order of 10−100 ppm and even if these impurities are significantly smaller than the channel dimensions. The larger particles act as nuclei for the aggregation and they are surrounded mostly by small nanoparticles, forming large agglomerates clogging the microchannels.[32] This phenomenon has been observed even for commercial suspensions with extended shelf life, and it has been identified to cause trouble in filtration, dispensing, or coating operations. A novel equipment called ring slit device has been introduced recently to examine flow-induced aggregation and to characterize the stability of concentrated suspensions exposed to strong flow fields. It has been used not only for industrial quality control and product development purposes, but also for systematic investigations on the heterocoagulation phenomenon mentioned.[32,33]

The ring-slit device embodies a capillary rheometer and ring-slit die. This setup allows a small gap height (10−30 μm), corresponding to a high contraction ratio (≈1:1000) and a large cross-sectional area at the same time. When aggregation takes place, the slit entrance is gradually clogged and this results in a strong pressure increase. Flow conditions can be varied in a wide range and thus can be adapted to match the specific flow process. Variation of the volumetric flow rate, slit height, and entrance angle allows to control the collision frequency and contact time of colliding particles, as well as the total deformation of a fluid element and the velocity gradient in the converging flow region where the aggregation takes place.

Here, we discuss the inkjet printing behavior of colloidal suspensions of inorganic, semiconductive particles. Aqueous formulations of commercial zinc oxide (ZnO) nanoparticles stabilized by a polyelectrolyte-type dispersing agent were used as a model system and printing experiments were performed on a commercial inkjet printer. Suspension stability and inverse Ohnesorge number Z (=Oh^{-1}) were systematically varied over a wide range. These investigations clearly reveal that flow-induced heterocoagulation due to a small fraction (≈100 ppm) of larger aggregates can cause severe problems during inkjet printing, even if Z is in an appropriate range for jetting of Newtonian fluids.

The present paper is organized as follows. The model suspensions, the characterization methods, and the experimental apparatus are described in the experimental part. Then, results are presented and discussed in terms of two issues: (1) ink jettability and (2) stability in converging flow fields. In the former, jetting behavior is explored according to various Z ranges, and in the latter, the relationship between flow-induced aggregation and clogging phenomena is discussed in terms of results both from ring-slit device and inkjet printer experiments. Finally the ideas are addressed regarding ink formulation and nozzle design that help to suppress nozzle clogging.

EXPERIMENTAL SECTION

Materials. A commercial ZnO powder (VP ADnano ZnO, Evonik degussa) with an active surface of 20−25 m^2/g and a density of 5.6×10^3 kg/m^3 was used in this investigation. The primary particles of ZnO powder were in the range of 20 nm, but they practically never isolated and typically formed aggregates, whose effective size was on the order of 100 nm (according to the manufacturer). Distilled water was used as a

suspending medium, and a commercial copolymer (Tego Dispers 752W, Evonik Tego Chemie) was used as a stabilizer (in the following we will refer to it as 'Tego' for simplicity). It consists of an anionic carboxylated backbone and nonionic polyglycol side chains.[9,34,35] Dispersions were prepared by adding ZnO solid particles into distilled water with different amounts of stabilizer, which was specified by its mass ratio relative to the net weight of ZnO. When the ZnO is immersed in water the surface of the oxide is hydrolyzed and a hydroxide layer is built up.[36] Due to the amphoteric properties of ZnO, it has positive charge under basic conditions when Tego is added to the system, and hydrogen bonding interactions between hydroxyl groups ($-Zn-(OH)^{2+}$) of ZnO and oxygen atoms ($-O-$) of the polyglycol of Tego lead to the adsorption of the stabilizer on the particle surface. Finally, ZnO nanodispersions are electrosterically stabilized by the anionic part of copolymer backbone. The pH dependence of the zeta potential of the neat and the polymer-stabilized ZnO dispersion is shown in Figure 1a. The neat ZnO shows an isoelectric point (IEP) at a pH of 10.0. The 'ZnO/polymer (Tego)' nanodispersion has an equilibrium pH of 9.0 and a zeta (ζ)-potential of -27 mV and has its IEP at pH of about 7.0.

The average particle size of these ZnO dispersions strongly depends on dispersing conditions. Here, dispersing was aided by ultrasonic treatment using a horn-type ultrasonicator (Digital Sonifier, Brason, U.S.A.). The effect of this ultrasonic treatment is demonstrated for a dispersion of ZnO 2 vol % with Tego/ZnO (w/w) = 0.10 in Figure 1b. The average particle diameter, as determined by dynamic light scattering, decreases with increasing ultrasonic treatment time (at a constant input power of 32 W) until it finally levels off at about 90 nm after 60 min. Accordingly, all nanodispersions investigated here have been exerted to this ultrasonic treatment procedure. Then they were filtrated with a mesh size of 5 μm (subsequently termed coarse filtration) before printing, unless otherwise stated. Sedimentation can be a problem in long-term storage, but the effect was not significant in our experiments. The inks were used up within one day after preparation, and they were mixed well; they were agitated for a few minutes with a magnetic stirrer and sonicated for 10 min just before performing the experiments.

To see the influence of the micrometer-sized fraction of aggregates on printing performances, some of the samples for inkjet printing experiments were additionally filtered with 0.45 and 1 μm syringe filters (Acrodisc) (subsequently termed fine filtration) Analogously, samples prepared for the ring slit tests described below were filtered with synthetic woven nanofilament fabric type filters (Sefar NITEX) having mesh sizes of 6 μm (coarse filtration) and 1 μm (fine filtration), respectively. These latter filters were chosen for convenience since ring slit tests require a larger amount of sample (150 mL) compared to inkjet printing experiments (usable ink capacity: up to 1.5 mL).

Characterization. Rheological measurements were carried out with a strain-controlled ARES rheometer (TA Instruments, U.S.A.) at shear rate $\dot{\gamma}$ ranging from 1 to 10^3 s^{-1} with cone–plate fixture (gap angle = 0.04 rad, diameter = 50 mm). Surface tension was measured by DCAT tensionmeter (DataPhysics Instruments GmbH, Germany). ζ-potential was measured with an AcoustoSizer IIs (Colloidal Dynamics Pry Ltd., Australia) as a function of pH with titration by using 1 M of HCl and 1 M of NaOH.

Two kinds of devices were used for particle sizing; the Zetasizer Nano ZS (Malvern Instruments Ltd., U.K.), which operates on the principle of dynamic light scattering (DLS), was used to determine the average particle diameter (measurement range 0.3–10 μm); the AccuSizer 780A (PSS, Inc., Santa Barbara, U.S.A.) equipped with a model LE400-05ES particle sensor, which is based on a single particle optical sensing technique (SPOS) counting individual objects in the range 0.5–400 μm, was used to determine the size distribution and total amount of particles/aggregates larger than 0.5 or 1 μm. Data collection was provided by the CW788-Nicomp software (PSS, Inc., Santa Barbara, CA), which accumulates the data in 512 logarithmically spaced channels from minimum to maximum size. The particle size assigned to a certain channel corresponds to the amplitude of the measured electrical pulse, and together with the number of particle counts for each channel, the total volume of particles in a selected range can be calculated. This technique is especially suitable for detecting and characterizing small fractions of objects larger than the primary particles.[37]

All measurements were carried out at room temperature.

Experimental Apparatus. *Inkjet Printer.* To observe the jetting behavior of ZnO dispersions, the commercial inkjet printer (DMP-2800, FUJIFILM Dimatix Inc., U.S.A.) was used with a 10 pL cartridge, which consists of 16 nozzles (DMC-11610). The smallest area the fluid passes in a cartridge is a circular cross-section with 21.5 μm diameter (according to the manufacturer); a schematic drawing is shown in Figure 2a.

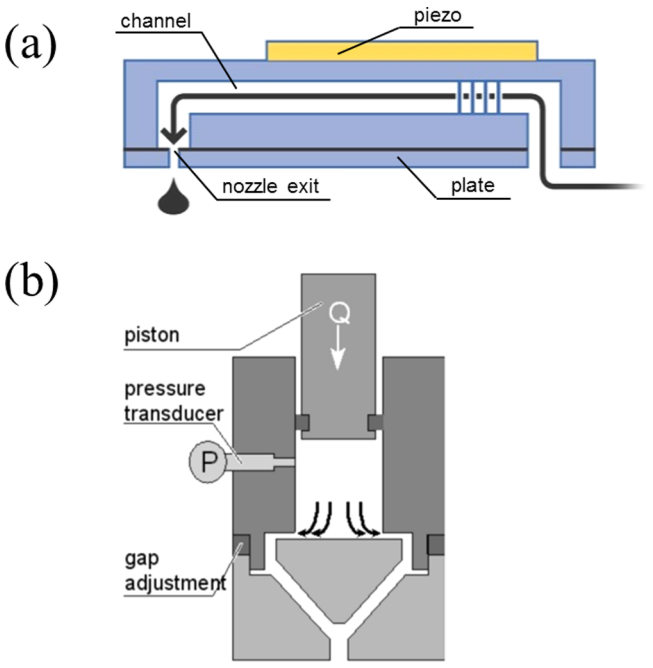

Figure 2. Schematic diagrams of (a) inkjet printer and (b) ring-slit device. Both apparatuses include a contraction channel.

Drops were generated by shear mode actuators based on the reverse piezoelectric effect and observed by a stroboscopic method using LED light for synchronization. We could capture the images of moving drops from the nozzle by changing the delay time between the pulse inception and the flash of LED light. In most cases inkjetting experiments were conducted at a driving voltage of 25 V (maximum applicable voltage is 40 V according to device specification, but for driving electronics a driving voltage of less than 40 V is preferred.).

Table 1. Characteristics of the Prepared Fluids

particle		stabilizer	material property			printing performance
ZnO (vol %)	continuous phase	Tego[a]/ZnO (w/w)	η (m Pa/s)	σ (m N/m)	Z (= Oh^{-1})	16 nozzles
2	water	0.1	1.2	63.1	30	misfiring
		0.5	1.7	55.2	20	jetting (very stable)
	G/W[b,g](20/80)	0.1	2.2	62.5	16	jetting
	DPG/W[c,g](5/95)	0.1	1.3	55.3	26	jetting
10	water	0.05	2.2	63.6	$^{(\dagger)}$16	clogging
		0.1	5.4	60.0	6.6	jetting
		0.5	13.2	55.2	2.5	jetting
	G/W[d](32/68)		2.4	68.0	†16	jetting
20	water	0.05	10.7	63.0	$^{(*)}$3.4	clogging
		0.1	25.8	59.9	$^{(\ddagger)}$1.4	nonjetting
	G/W[e](62/38)		11.2	65.0	$^{(*)}$3.4	jetting
	G/W[f](76/24)		29.0	61.9	$^{(\ddagger)}$1.4	nonjetting

[a]Tego Dispers 752W, a copolymer consisting of polycarboxylate ether in water at a concentration of 50 wt %, free of amino groups, hydroxyl groups, and nonyl phenol ethoxylates.[9] [b]G/W(20/80): The continuous phase was changed as glycerol(G)−water(W) mixture (20%/80%) for adjusting Z. [c]DPG/W(5/95): The continuous phase was changed as dipropyleneglycol(DPG)−water(W) mixture (5%/95%) for adjusting Z. [d]G/W(32/68): Newtonian reference of glycerol(G)−water(W) mixture (32%/68%) for clogging analysis. The value of Z is equivalent with that of ZnO 10 vol % with Tego/ZnO = 0.05 ($^{(\dagger)}Z$ = 16). [e]G/W(62/38): Newtonian reference of glycerol(G)−water(W) mixture (62%/38%) for clogging analysis. The value of Z is equivalent with that of ZnO 20 vol % with Tego/ZnO = 0.05 ($^{(*)}Z$ = 3.4). [f]G/W(76/24): Newtonian reference of glycerol(G)−water(W) mixture (76%/24%) for not-jetting analysis. The value of Z is equivalent with that of ZnO 20 vol % with Tego/ZnO = 0.1 ($^{(\ddagger)}Z$ = 1.4). [g]In material property, viscosity is more changeable by glycerol(G) addition, while surface tension is more susceptible by dipropylene glycol(DPG) addition.

Ring-Slit Device. A ring-slit device was used to characterize flow-induced aggregation. We used the setup that has been described in detail earlier;[32,33] a schematic drawing is shown in Figure 2b. The ring-slit device includes a capillary rheometer (Rosand RH2000, Malvern U.K.) and a homemade stainless steel ring-slit die. The ring-slit height H is fixed as (23 ± 1) μm in order to match with nozzle size (21.5 μm) of the inkjet printer. This corresponds to a contraction ratio of 1:1000 between the diameter of the sample chamber and the slit height. The sample is forced to flow through the ring-shaped slit with a constant volumetric flow rate Q, which is controlled by setting the piston speed v. A pressure transducer mounted above the die records the corresponding extrusion pressure p as a function of time or extruded sample volume.

If the suspension is stable, the pressure adjusts itself to a comparably low constant value determined by the viscosity of the particular sample. In this case, the instrument operates as a high shear capillary rheometer and the apparent shear rate $\dot{\gamma}_{app}$, apparent shear stress τ_{app}, and viscosity η_{app} can be calculated as follows:[37]

$$\dot{\gamma}_{app} = \frac{6Q}{BH^2} \text{ with } Q = \pi R^2 v \quad (1)$$

$$\tau_{app} = \frac{p}{2L/H} \quad (2)$$

$$\eta_{app} = \frac{\tau_{app}}{\dot{\gamma}_{app}} \quad (3)$$

where R = 12 mm is the radius of the sample chamber, $B = 2\pi R$, and L = 1 mm is the length of the ring-slit. If the suspension is not stable, aggregates gradually clog the slit and the extrusion pressure increases with time. The recorded pressure signal is normalized by the so-called viscous pressure $p_{viscous}$, which is set equal to the initial pressure reading corresponding to the viscosity of the suspension, so that we only compare the pressure increase caused by the flow-induced aggregation.

Experiments have been done at two different flow rates, 63 mm^3/s and 1574 mm^3/s, as well as two different entrance angles, 45° and 90°, in order to see the effect of flow kinematics and hydrodynamic force on slit clogging. All experiments were conducted at room temperature.

RESULT AND DISCUSSION

Ink Jettability. The aim of this study is to tailor printable nanoinks for drop-on-demand inkjet printing. From a fluid mechanics point of view, viscosity η and surface tension σ of the dispersions should be controlled. Viscosity contributes to drop formation by induced pressure wave propagation inside the nozzle, and surface tension contributes to the pinch-off of drops at the nozzle exit. To project droplet at the nozzle orifice, the action of the pressure wave should break the barrier of surface tension.

First of all, to set the various ranges of $Z = Oh^{-1} = Re/We^{1/2} = (d\rho\sigma)^{1/2}/\eta$, the amount of ZnO particles and dispersant Tego were changed. ZnO was added into the distilled water by 2, 10, and 20 vol %, and then, Tego was added by 5−50 wt % in reference to ZnO. For the prepared ZnO suspensions, η, σ, and the dimensionless number Z are summarized in Table 1, together with a short comment on printing performance. Viscosity of the prepared ZnO suspensions is shown in Figure 3. Most of the suspensions showed constant viscosity independent of shear rate, but the suspensions with 20 vol % ZnO exhibited slight shear thinning. In this case, the entries in Table 1 correspond to shear rates of 1000 s^{-1}.

According to previous literature,[22,38−43] Z is the decisive parameter for judging the jettability in inkjet printing. When Z is too low, drops are not generated due to energy dissipation in the nozzle, while satellite drops are formed during printing when Z is too high. Strictly speaking this criterion can be applied only to Newtonian fluids, while additional concepts should be considered to deal with the jetting performance of particulate suspensions, which include nanoparticles and stabilizers.

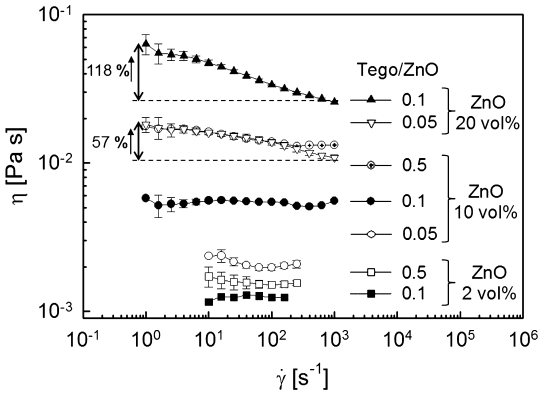

Figure 3. Viscosities of the ZnO suspensions as a function of shear rate.

The viscosity values obtained can be used to calculate a Péclet number (Pe) for the inkjet printing process to judge the relevance of applied shear forces:

$$\mathrm{Pe} = \frac{\text{Flow force}}{\text{Brownian force}} = \frac{\dot{\gamma}_{\mathrm{wall}}}{k_{\mathrm{B}}T/(6\pi\eta a^3)} \tag{4}$$

where k_{B}, T, and η are the Boltzmann constant (1.38×10^{-23} J/K), the temperature (278 K), and the fluid viscosity, respectively. The wall shear rate $\dot{\gamma}_{\mathrm{wall}}$ at the nozzle exit can be calculated from the average drop velocity $\langle v_x \rangle$, (this quantity depends linearly on the driving voltage, and 25 V corresponds to an average drop velocity of about 5 m/s):

$$\dot{\gamma}_{\mathrm{wall}} = \left.\frac{\mathrm{d}v_x}{\mathrm{d}r}\right|_{\mathrm{wall}} = \frac{4Q}{\pi R^3}, \quad \text{with } Q = \pi R^2 \langle v_x \rangle \tag{5}$$

assuming Newtonian flow behavior. Here, R and a denote nozzle orifice diameter (21.5 μm) and average particle size (85 nm), respectively. Finally, inserting typical values for the suspensions investigated here results in Pe $\approx$ 100−1000, and this implies that the fluids experience strong flow in inkjet printing.

ZnO 2 vol % Suspensions. Inkjet printing experiments were conducted for different $Z = (d\rho\sigma)^{1/2}/\eta$ values. Z was varied using different glycerol/water and dipropylenglycol/water mixtures (see Table 1).

For 2 vol % ZnO and Tego/ZnO = 0.1 with Z = 30 lots of directional misfiring spray, and very different drop velocities among the 16 nozzles operating simultaneously were observed, as shown in Figure 4a. However, upon changing Z to Z = 16

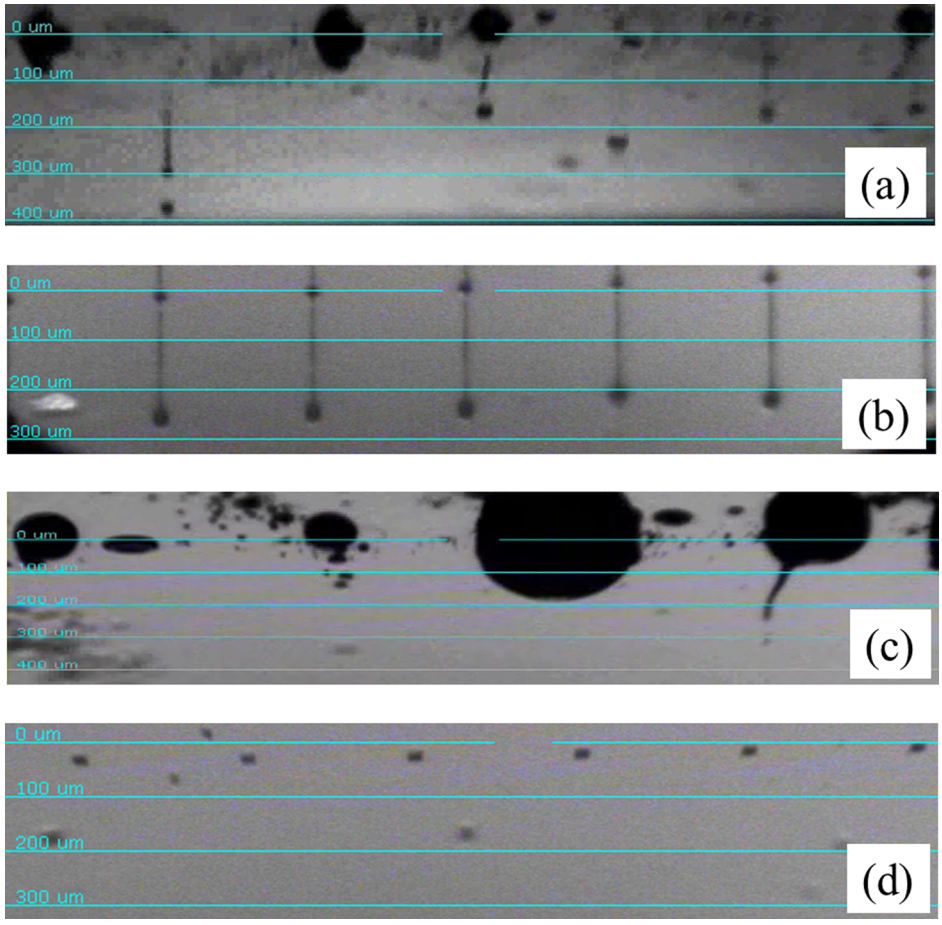

Figure 4. Typical jetting behaviors: (a) misfiring, (b) stable drop-jetting, (c) nozzle clogging, and (d) nonjetting. (a) The suspension with 2 vol % ZnO and Tego/ZnO = 0.1 (Z = 30) showed dissimilar drop velocities and lots of directional misfiring; (b) the suspension of 2 vol % ZnO and Tego/ZnO = 0.5 (Z = 20) resulted in stable drop-jetting in all nozzles; (c) the suspension with 10 vol % ZnO and Tego/ZnO = 0.05 (Z = 16) showed nozzle clogging and never good drop jetting behavior; (d) the suspension with 20 vol % ZnO and Tego/ZnO = 0.1 (Z = 1.4) did not jet from the beginning.

dx.doi.org/10.1021/ie301403g | *Ind. Eng. Chem. Res.* 2012, 51, 13195−13204

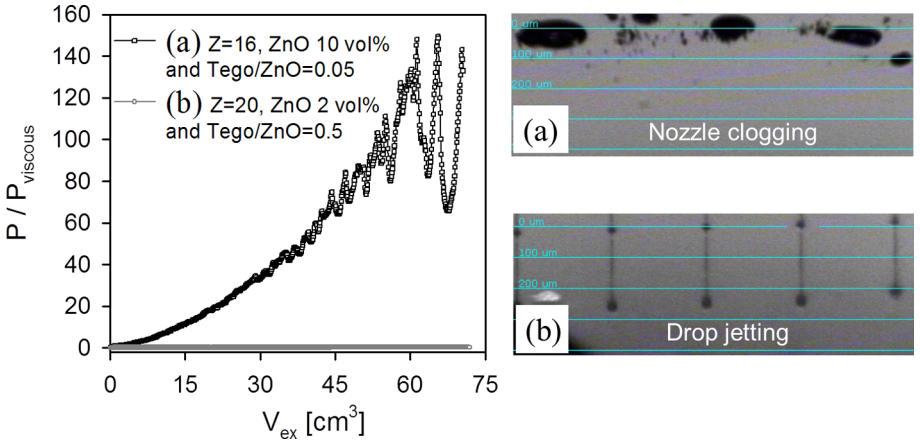

Figure 5. Comparison of flow behavior in ring-slit device (left) and inkjet printer (right) for the suspensions of similar, intermediate Z values (Z = 16 and Z = 20). (a) The suspension that shows nozzle clogging exhibits a dramatic pressure increase, while (b) the suspension that shows stable drop-jetting shows a constant pressure signal.

and Z = 26 by variation of the solvent, stable drops were ejected.

The system with 2 vol % ZnO and Tego/ZnO = 0.5 (Z = 20) also exhibited stable drop-jetting, as shown in Figure 4b. Moreover, this system was so well-stabilized that a constant drop velocity was obtained at all nozzles.

These findings reveal that an appropriate intermediate Z range is advantageous for inkjet printing as expected, but even if Z is in the proper range printing, results can be further improved if the colloidal stability of the suspensions is increased (e.g. due to the addition of suitable surfactants).

ZnO 10 vol % Suspensions. Inkjet printing experiments were conducted using 10 vol % ZnO suspensions with Tego/ZnO ratios of 0.5 (Z = 2.5) and 0.1 (Z = 6.6). Both suspensions did show good printing results over an extended period of time despite their low Z values.

In contrast, the suspension with the same ZnO concentration but lower Tego/ZnO ratio of 0.05 (Z = 16) exhibited poor jetting for a short period of time, but drops were not ejected anymore after this initial period. In addition, the system did show wetting around the nozzle and accumulation of printed material, as shown in Figure 4c. In order to confirm that Z = 16 is in the appropriate range for printing, a glycerol/water mixture (32%/68%) with Z = 16 was used as a Newtonian reference, and it was printable perfectly. We suppose that the nonjetting phenomenon is caused by nozzle clogging due to the existence of aggregates or other impurities. Therefore, we conducted fine filtration (with mesh sizes of 0.45 and 1 μm) for the suspension with 10 vol % ZnO and Tego/ZnO = 0.05 (Z = 16), and then observed that the drops were ejected without clogging.

Based on these observations, we conclude that even if Z is in the appropriate jettable range drops might not be formed due to nozzle clogging. Furthermore, we hypothesize that extant micrometer-sized impurities act as nuclei for aggregation in the flow field at the nozzle exit.

This will be discussed in more detail below.

ZnO 20 vol % Suspensions. Due to the high particle loading, the viscosity of these suspensions is high, and accordingly, Z is low. Moreover, these suspensions exhibit shear thinning. For the suspensions with Tego/ZnO = 0.05 (Z = 3.4) and Tego/ZnO = 0.1 (Z = 1.4), drops were not ejected at all, as shown in Figure 4d, even when a maximum voltage of 40 V was applied. To investigate the nonjetting phenomenon observed during printing, glycerol/water mixtures with similar Z values (see Table 1) were used as Newtonian reference fluids. For the Z = 3.4, fluid drops were ejected very well. For Z = 1.4, the fluid did not jet at a voltage of 25 V, while it did show drop-jetting at a driving voltage of 40 V for a while, but showed shutoff of the nozzle in the long run, and also did not recover when trying to operate the inkjet printer again.

For the suspension with Z = 1.4, three possible mechanisms for nonjetting actuation are suggested here. First, the low value of Z corresponds to a high suspension viscosity, which results in a dissipation of the pressure pulse and thus prevents drop-jetting.[26] Second, nonjetting might be due to dipole-like flow (doublet flow) caused by a vibrating meniscus. The cause of dipole-like flow is not clear yet, but acoustic streaming by capillary waves or local interfacial tension distortion can be regarded as the origin.[44,45] Third, when air bubbles are entrapped in the ink, surface tension increases so that drops are not ejected even when a large amplitude driving voltage is applied.[44,46]

For the 20 vol % ZnO suspension with Tego/ZnO = 0.05 and Z = 3.4, we assume that the observed nozzle clogging is due to flow-induced aggregation resulting from an insufficient colloidal stability, similar to the case of the 10 vol % ZnO suspension with Z = 16.

In conclusion, our investigations reveal that for ZnO suspensions drops may be ejected from an inkjet printer if Z is in the range $2.5 < Z < 26$. However, in contrast to Newtonian fluids or weakly viscoelastic polymer solutions, this criterion is not sufficient. For certain suspensions, nonjetting and nozzle clogging were observed presumably due to flow-induced aggregation at the nozzle exit. This may happen if the suspended nanoparticles are not sufficiently stabilized, and aggregation may be promoted by a small fraction of impurities or aggregates much larger than the primary particles, but still smaller than the nozzle diameter of the printer. This hypothesis will be discussed in detail in the next section.

Stability in Converging Flow Fields. *Validation of Flow Similarity between Ring-Silt Device and Inkjet Printer.* We have studied the stability and flow-induced aggregation in contraction flow using a ring-slit device, which was operated under similar conditions as the inkjet printer regarding flow velocity v_x and slit height H or nozzle diameter D. First of all, to

dx.doi.org/10.1021/ie301403g | Ind. Eng. Chem. Res. 2012, 51, 13195−13204

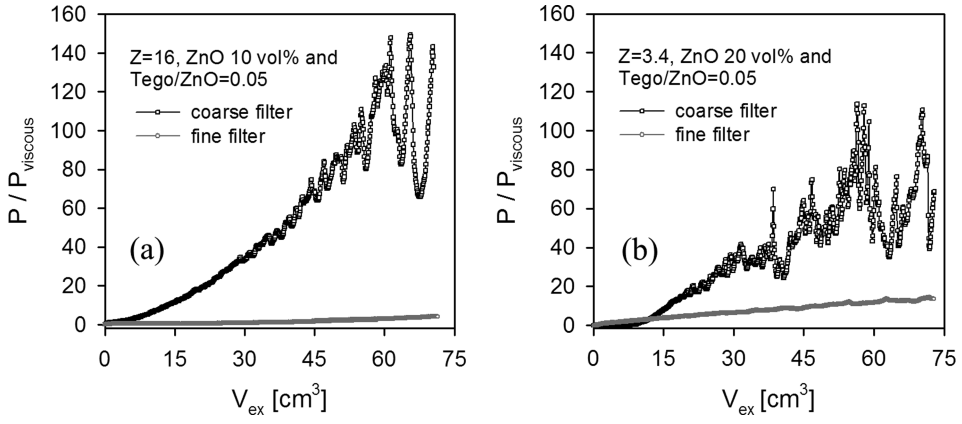

Figure 6. (a) Effect of filtration efficiency on pressure development for suspensions with (a) 10 vol % ZnO and Tego/ZnO = 0.05 (Z = 16) and (b) 20 vol % ZnO and Tego/ZnO = 0.05 (Z = 3.4) at flow rate = 63 mm^3/s.

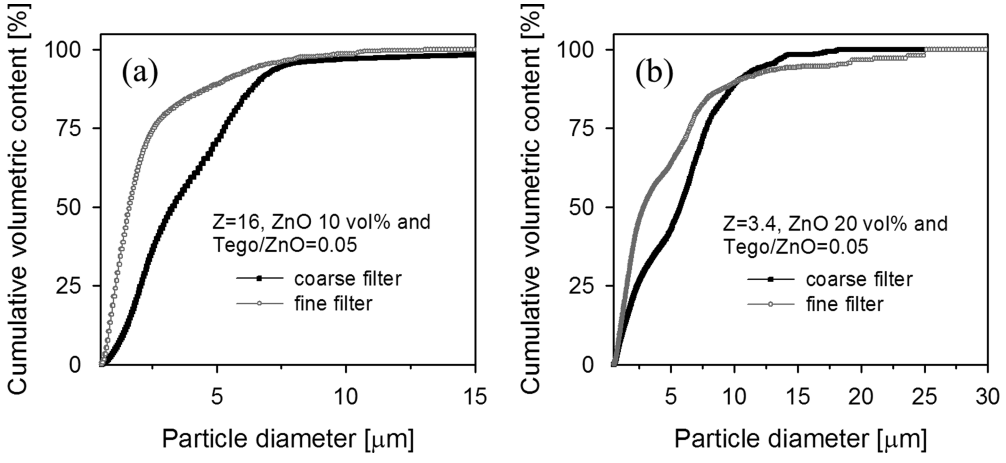

Figure 7. Cumulative volumetric distributions of micrometer-sized particles for suspensions with (a) 10 vol % ZnO and Tego/ZnO = 0.05 (Z = 16) and (b) 20 vol % ZnO and Tego/ZnO = 0.05 (Z = 3.4) by single particle optical sensing (SPOS) technique.

validate the flow similarity between these two types of apparatus, namely the inkjet printer and the ring-slit device, the output performance for two suspensions of similar intermediate Z ranges (Z = 16 and Z = 20) was compared. As a result, the suspension that formed stable drop-jetting in inkjet printing did show a constant pressure signal in the ring-slit test, while the suspension that caused nozzle clogging in inkjet printing exhibited a dramatic pressure increase in the ring-slit test. In other words, the flow similarity in these two apparatus was verified reasonably (see Figure 5). At a driving voltage of 25 V, wall shear rates $\dot{\gamma}_{wall}$in the nozzle are on the order of 10^5 s^{-1}. The shear rate in the slit channel depends on the applied piston speed; it corresponds to 11 000 s^{-1} at a flow rate of 63 mm^3/s and 280 000 s^{-1} at a flow rate of 1574 mm^3/s (eq 1). According to Wang et al.,[12] the shear rate in the nozzle is on the order of 10^5 s^{-1} for the first few microseconds but then quickly drops to 10^4 s^{-1} after about 15 μs. Thus, we think the deformation rates in both devices are matched well.

Flow-Induced Aggregation in Slit and Nozzle Entrance. In the light of previous investigations on concentrated polymer dispersions,[32] we anticipate that nozzle clogging observed for the ZnO suspensions in inkjet printing is a result of flow-induced aggregation, and this phenomenon is promoted by a small fraction of micrometer-sized impurities.

To demonstrate the effect of such impurities or aggregates on clogging, pressure profiles were examined for suspensions with Z = 16 and Z = 3.4 (which led to nozzle clogging) prefiltered with different mesh sizes (coarse (6 μm) and fine (1 μm) filter), as shown in Figure 6. The coarse filtered suspensions did show strong pressure increase, while the fine filtered suspensions exhibited only a weak, linear pressure increase. From these results, we conclude that aggregates in the size range between 1 and 6 μm are decisive for the observed clogging phenomenon.

This is in line with previous investigations revealing that the number density of particles larger than 0.5 or 1 μm is a crucial factor that may cause trouble during jetting.[47]

We have investigated the colloidal stability of ZnO suspensions using a single particle optical sensing (SPOS) technique. This technique is used to characterize the size distribution and total amount of extant impurities/aggregates larger than 0.5 or 1 μm quantitatively, which are supposed to be decisive parameters for nozzle clogging.

Results for the suspensions with 10 vol % ZnO and Tego/ZnO = 0.05 as well as 20 vol % ZnO and Tego/ZnO = 0.05, which exhibited slit clogging are shown in Figure 7. Prefiltration with the fine filter shifted the particle size distribution to lower values compared to the coarse filtration as expected.

The measured values for the fraction of aggregates larger than 1 μm $\varphi_{aggregates} = V_{aggregates}/V_{dispersion}$ normalized by the total volume fraction of solids $\varphi_{initial}$ as well as the total number of particles larger than 1 μm found in different suspensions are

dx.doi.org/10.1021/ie301403g | Ind. Eng. Chem. Res. 2012, 51, 13195−13204

Table 2. Quantitative Analysis of Aggregates for ZnO Suspensions by SPOS Technique

ZnO in vol %	2		10					20
	0.1	0.5	0.05			0.1	0.5	0.1
*m*Tego/*m*ZnO (w/w)	w/o filter	w/o filter	w/o filter	coarse filter	fine filter	w/o filter	w/o filter	w/o filter
$(\phi_{aggregates}/\phi_{initial})\times 10^{-6}(\geq 1\ \mu m)$	315	260	620	500	360	560	360	830
no. aggregates ($\geq 1\ \mu m$) (10^5 aggregates/$mL_{dispersion}$)	2.32	2.01	7.42	7.11	4.86	6.43	6.85	18.3

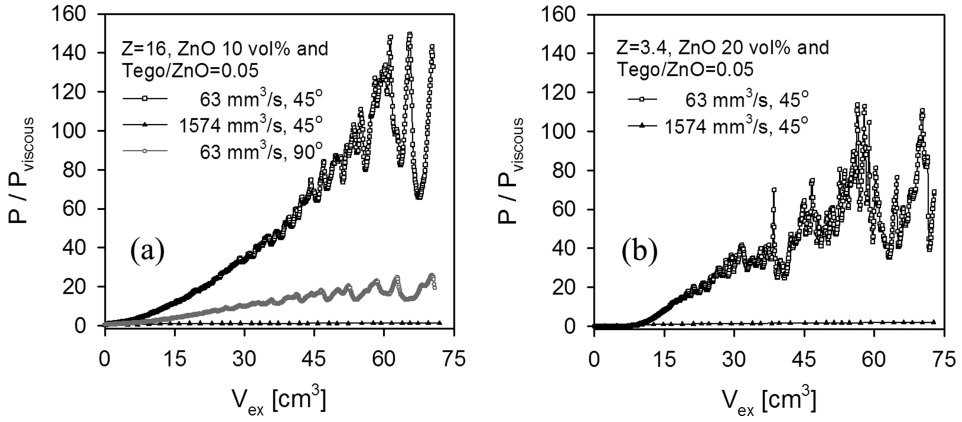

Figure 8. Effect of flow rate and entrance angle on flow-induced aggregation for suspensions with (a) 10 vol % ZnO and Tego/ZnO = 0.05 ($Z = 16$) and (b) 20 vol % ZnO and Tego/ZnO = 0.05 ($Z = 3.4$).

summarized in Table 2. As expected, the relative volume fraction and the number of aggregates increase with increasing solids content. At fixed ZnO concentration the relative volume fraction and number of aggregates decreases with increasing amount of stabilizer. Finally, the relative volume fraction and number of aggregates decreases with decreasing filter mesh size at fixed ZnO and stabilizer concentration.

These results from SPOS analysis are as expected, and they further confirm that the fraction and number of aggregates in the micrometer range is crucial for nozzle clogging during inkjet printing. For the ZnO suspensions investigated here, the relative volume fraction of aggregates $\geq 1\ \mu m$ should not exceed 500 ppm and their total number should be below 7×10^5/mL in order to avoid clogging.

Now the question remains whether nozzle clogging is due to flow-induced homocoagulation between micrometer-sized impurities or heterocoagulation between these impurities. This phenomenon has been investigated carefully for a series of different concentrated polymer dispersions, and it could be clearly shown that heterocoagulation is the mechanism controlling nozzle clogging in these systems.[32] The most important argument, which also holds for the ZnO suspensions investigated here, is that the collision probability between micrometer-sized impurities is extremely low, since it is proportional to their concentration squared. Therefore, homocoagulation of the large objects is unlikely. We, therefore, propose that heterocoagulation takes place between micrometer-sized impurities and nanoparticles of ZnO in the elongational flow field at the nozzle exit (similar to that observed by Georgieva et al.[32]), even if the size of these impurities is smaller than the size of the nozzle gap or slit height, and that this is the origin of nozzle clogging finally preventing proper inkjet printing.

To examine the flow-induced aggregation mechanism from a perspective of processing conditions, the effects of flow rate and entrance angle on extrusion through the ring-slit device were investigated for two suspensions that exhibited clogging phenomena in inkjet printing. The corresponding results are shown in Figure 8. For both suspensions, the pressure increase was much more pronounced at the lower flow rate (63 mm^3/s) and an almost stable pressure signal was observed at the higher flow rate (1574 mm^3/s). These results further support that nozzle clogging is not due to hydrodynamic bridging (clogging would then be more pronounced at higher flow rate) but by flow-induced aggregation. Applying higher flow rates results in a break-up of aggregates and might be compared with a purging process where large air pressure is applied to remove residual impurities inside the nozzle. The entrance angle also had a strong effect on slit clogging, as can be seen from Figure 8a. The larger entrance angle (90°) resulted in a better stability than a smaller entrance angle (45°). This is in line with the results already reported[32] and may be attributed to the shorter time of exposure to the elongational flow field, which is especially relevant for well-stabilized systems, where particles need a certain minimum contact time in order to form aggregates.

■ CONCLUSIONS

The drop jettability during inkjet printing has been investigated for zinc oxide (ZnO) particulate suspensions. In analogy to the approach for judging the drop formation properties of Newtonian fluids the dimensionless number Z as an inverse Ohnesorge number, Oh^{-1} was introduced to the range of printability in dependence of viscosity, surface tension, and density of the inks. For the inkjet printing setup used here, we could demonstrate that jetting was possible without any problem for Newtonian fluids as long as $2.5 < Z < 26$, but in the identical range, nonjetting occurred due to nozzle clogging for certain colloidal ZnO suspensions, and this is attributed to flow-induced aggregation in the contraction zone at the nozzle exit.

This flow-induced aggregation phenomenon was further investigated using a so-called ring-slit device. This device allows for simultaneous formation and detection of aggregates in strongly converging flow fields and is operated here under similar conditions as the inkjet printer regarding flow velocity v_x and slit height H or nozzle diameter D.

We could show that the pressure increase during extrusion of the suspension through the ring-slit is correlated to the nozzle clogging observed in inkjet printing. Our experiments suggest that the flow-induced aggregation is promoted by a small fraction of micrometer-sized aggregates acting as nuclei for heterocoagulation with the nanoscale suspension particles in the contraction zone. Especially, the aggregates in the size range between 1 and 6 μm are decisive imparting nozzle clogging thereby preventing proper inkjet printing, even though the size of these aggregates is smaller than the size of the nozzle cross-section. The relative volume fraction of aggregates, $\varphi_{\text{aggregates}}/\varphi_{\text{initial}} \geq 1$ μm, should not exceed 500 ppm, and their total number should be below 7×10^5/mL in order to avoid nozzle clogging. Flow-induced aggregation can also be suppressed by appropriate stabilization of the nanoparticles, but this is often not achievable without impairing the electric performance of the printed structure. From a processing or printing head design perspective, clogging probability can be reduced either by applying a higher driving voltage, which corresponds to a higher flow rate, or by optimizing the contraction zone such that the exposure time of the ink to the elongational flow field is reduced. The former results in a break-up of existing or previously formed aggregates; the latter corresponds to a lower probability of aggregate formation.

Finally, this study clearly reveals that besides the classical inverse Ohnesorge number criterion additional colloidal stability parameters have to be considered in order to optimize suspension based printing inks for inkjet printing purposes and that the printing process parameters and nozzle design may have to be adjusted in order to establish this promising technology for low cost manufacturing of electronic devices.

AUTHOR INFORMATION

Corresponding Author

*Tel.: +49 721 608 42661. Fax: +49 721 608 43758. E-mail: norbert.willenbacher@kit.edu.

Notes

The authors declare no competing financial interest.

ACKNOWLEDGMENTS

This work was supported by the National Research Foundation of Korea (NRF) grant (No. 20100026139) funded by the Korea government (MEST). A. Lee acknowledges a Visiting Researcher Scholarship from Karlsruhe Institute of Technology (KIT).

REFERENCES

(1) Jeong, S.; Kim, D.; Moon, J. Ink-Jet-printed organic−inorganic hybrid dielectrics for organic thin-film transistors. *J. Phys. Chem. C* **2008**, *112*, 5245−5249.

(2) Sirringhaus, H.; Kawase, T.; Friend, R. H.; Shimoda, T.; Inbasekaran, M.; Wu, W.; Woo, E. P. High-resolution inkjet printing of all-polymer transistor circuits. *Science* **2000**, *290*, 2123−2126.

(3) Kim, S.; Kim, J. H.; Ahn, K. H.; Lee, S. J. Rheological perspectives of industrial coating process. *Korea-Aust. Rheol. J.* **2009**, *21*, 83−89.

(4) Bubel, S.; Nikolova, D.; Mechau, N.; Hahn., H. Influence of stabilizers in ZnO nanodispersions on field-effect transistor device performance. *J. Appl. Phys.* **2009**, *105*, 064514.

(5) Dasgupta, S.; Gottschalk, S.; Kruk, R.; Hahn, H. A nano-particulate indium tin oxide field-effect transistor with solid electrolyte gating. *Nanotechnology* **2008**, 435203.

(6) Mathews, N.; Lam, Y. M.; Mhaisalkar, S. G.; Grimadale, A. C. Printing materials for electronic devices. *Int. J. Mat. Res.* **2010**, *101*, 236−250.

(7) Mechau, N.; Bubel, S.; Nikolova, D.; Hahn, H. Influence of stabilizers in ZnO nano-dispersions on the performance of solution-processed FETs. *Phys. Status Solidi A* **2010**, *207*, 1684−1688.

(8) Okamura, K.; Mechau, N.; Nikolova, D.; Hahn, H. Influence of interface roughness on the performance of nanoparticulate zinc oxide field-effect transistors. *Appl. Phys. Lett.* **2008**, *93*, 083105.

(9) Okamura, K.; Nikolova, D.; Mechau, N.; Hahn, H. Polymer stabilized ZnO nanoparticles for low-temperature and solution-processed field-effect transistors. *J. Mater. Chem.* **2010**, *20*, 5651−5658.

(10) Sun, Y.; Rogers, J. A. A. Inorganic semiconductors for flexible electronics. *Adv. Mater.* **2007**, *19*, 1897−1916.

(11) Habas, S. E.; Platt, H. A. S.; van Hest, M. F. A. M.; Ginley, D. S. Low-cost inorganic solar cells: From ink to printed device. *Chem. Rev.* **2010**, *110*, 6571−6594.

(12) Wang, X.; Carr, W. W.; Bucknall, D. G.; Morris, J. F. Drop-on-demand drop formation of colloidal suspensions. *Int. J. Multiphase Flow* **2012**, *38*, 17−26.

(13) Tsai, B.; Carvalho, M. S.; Kumar, S. Leveling of thin films of colloidal suspensions. *J. Colloid Interface Sci.* **2010**, *343*, 306−313.

(14) Maki, K. L.; Kumar, S. Fast evaporation of spreading droplets of colloidal suspensions. *Langmuir* **2011**, *27*, 11347−11363.

(15) Cardinal, C. M.; Jung, Y. D.; Ahn, K. H.; Francis, L. F. Drying regime maps for particulate coatings. *AIChE J.* **2010**, *56*, 2769−2780.

(16) Cibis, D.; Krüger, K. System analysis of a DoD print head for direct writing of conductive circuits. *Int. J. Appl. Ceram. Technol.* **2007**, *4*, 428−435.

(17) Kwon, K. S.; Kim, W. A waveform design method for high-speed inkjet printing based on self-sensing measurement. *Sens. Actuators A* **2007**, *140*, 75−83.

(18) Kwon, K. S. Waveform design methods for piezo inkjet dispensers based on measured meniscus motion. *J. Microelectromech. Syst.* **2009**, *18*, 1118−1125.

(19) Perelaer, J.; Smith, P. J.; Wijnen, M. M. P.; van den Bosch, E.; Eckardt, R.; Ketelaars, P. H. J. M.; Schubert, U. S. Droplet tailoring using evaporative inkjet printing. *Macromol. Chem. Phys.* **2009**, *210*, 387−393.

(20) Jang, D.; Kim, D.; Moon, J. Influence of fluid physical properties on ink-jet printability. *Langmuir* **2009**, *25*, 2629−2635.

(21) Jo, B. W.; Lee, A.; Ahn, K. H.; Lee, S. J. Evaluation of jet performance in drop-on-demand (DOD) inkjet printing. *Korean J. Chem. Eng.* **2009**, *26*, 339−348.

(22) Tai, J. Y.; Gan, H. Y.; Liang, Y. N.; Lok, B. K. Control of droplet formation in inkjet printing using Ohnesorge number category: Materials and processes. In *Proceedings of the 10th Electronics Packaging Technology Conference (ECTC2008)*, Singapore, 2008; pp 761−766.

(23) Tuladhar, T. R.; Mackley, M. R. Filament stretching rheometry and break-up behavior of low viscosity polymer solutions and inkjet fluids. *J. Non-Newtonian Fluid Mech.* **2008**, *148*, 97−108.

(24) Vadillo, D. C.; Tuladhar, T. R.; Mulji, A. C.; Jung, S.; Hoath, S. D.; Mackley, M. R. Evaluation of the inkjet fluid's performance using the "Cambridge Trimaster" filament stretch and break-up device. *J. Rheol.* **2010**, *54*, 261−282.

(25) Vadillo, D. C.; Tuladhar, T. R.; Mulji, A. C.; Mackley, M. R. The rheological characterization of linear viscoelasticity for ink jet fluids using piezo axial vibrator and torsion resonator rheometers. *J. Rheol.* **2010**, *54*, 781−795.

(26) Reis, N.; Ainsley, C.; Derby, B. Ink-jet delivery of particle suspensions by piezoelectric droplet ejectors. *J. Appl. Phys.* **2005**, *97*, 094903.

(27) Xie, D. L.; Wu, H.; Zaccone, A.; Braun, L.; Chen, H. Q.; Morbidelli, M. Criticality for shear-induced gelation of charge-stabilized colloids. *Soft Matter* **2010**, *6*, 2692−2698.
(28) Zaccone, A.; Wu, H.; Gentili, D.; Morbidelli, M. Theory of activated-rate processes under shear with application to shear-induced aggregation of colloids. *Phys. Rev. E* **2009**, *80*, 051404.
(29) Zaccone, A.; Gentili, D.; Wu, H.; Morbidelli, M. Shear-induced reaction-limited aggregation kinetics of Brownian particles at arbitrary concentrations. *J. Chem. Phys.* **2010**, *132*, 134903.
(30) Ramachandran, V.; Fogler, H. S. Plugging by hydrodynamic bridging during flow of stable colloidal particles within cylindrical pores. *J. Fluid Mech.* **1999**, *385*, 129−156.
(31) Wyss, H. M.; Blair, D. L.; Morris, J. F.; Stone, H. A.; Weitz, D. A. Mechanism for clogging of microchannels. *Phy, Rev. E* **2006**, *74*, 061402.
(32) Georgieva, K.; Dijkstra, D. J.; Fricke, H.; Willenbacher, N. Clogging of microchannels by nano-particles due to hetero-coagulation in elongational flow. *J. Colloid Interface Sci.* **2010**, *352*, 265−277.
(33) Ettl, R.; Schadler, V.; Willenbacher, N. Runnability and flow-induced aggregation of paper coating suspensions. *Nord. Pulp Pap. Res. J.* **2000**, *15*, 509−514.
(34) Sis, H.; Birinci, M. Effect of nonionic and ionic surfactants on zeta potential and dispersion properties of carbon black powders. *Colloids Surf., A* **2009**, *341*, 60−67.
(35) Hommer, H. Interaction of polycarboxylate ether with silica fume. *J. Eur. Ceram. Soc.* **2009**, *29*, 1847−1853.
(36) Degen, A.; Kosec, M. Effect of pH and impurities on the surface charge of zinc oxide in aqueous solution. *J. Eur. Ceram. Soc.* **2000**, *20*, 667−673.
(37) Remsen, E. E.; Anjur, S.; Boldridge, D.; Kamiti, M.; Li, S.; Johns, T.; Dowell, C.; Kasthurirangan, J.; Feeney, P. Analysis of large particle count in fumed silica slurries and its correlation with scratch defects generated by CMP. *J. Electrochem. Soc.* **2006**, *153*, G453−G461.
(38) Fakhfouri, V.; Mermoud, G.; Kim, J. Y.; Martinoli, A.; Brugger, J. Drop-on-demand inkjet printing of SU-8 polymer. *Micro Nanosyst.* **2009**, *1*, 63−67.
(39) Tekin, E.; Smith, P. J.; Schubert, U. S. Inkjet printing as a deposition and patterning tool for polymers and inorganic particles. *Soft Matter* **2008**, *4*, 703−713.
(40) Tafreshi, H. V.; Pourdeyhimi, B. The effects of nozzle geometry on waterjet breakup at high Reynolds numbers. *Exp. Fluids* **2003**, *35*, 364−371.
(41) McKinley, G. H. Dimensionless groups for understanding free surface flows of complex fluids. *Rheol. Bull.* **2005**, *74* (2), 6−10.
(42) Pilch, M.; Erdman, C. A. Use of Breakup Time Data and Velocity History Data to Predict the Maximum Size of Stable Fragments for Acceleration-Induced Breakup of a Liquid-Drop. *Int. J. Multiphase Flow* **1987**, *13*, 741−757.
(43) Perelaer, J.; Smith, P. J.; Mager, D.; Soltman, D.; Volkman, S. K.; Subramanian, V.; Korvink, J. G.; Schubert, U. S. Printed electronics: the challenges involved in printing devices, interconnects, and contacts based on inorganic materials. *J. Mater. Chem.* **2010**, *20*, 8446−8453.
(44) Beulen, B.; de Jong, J.; Reinten, H.; van den Berg, M.; Wijshoff, H.; van Dongen, R. Flows on the nozzle plate of an inkjet printhead. *Exp. Fluids* **2007**, *42*, 217−224.
(45) Marmottant, P.; Hilgenfeldt, S. Controlled vesicle deformation and lysis by single oscillating bubbles. *Nature* **2003**, *423*, 153−156.
(46) de Jong, J.; de Bruin, G.; Reinten, H.; van den Berg, M.; Wijshoff, H.; Versluis, M.; Lohse, D. Air entrapment in piezo-driven inkjet printheads. *J. Acoust. Soc. Am.* **2006**, *120*, 1257−1265.
(47) Shakhnovich, A.; Belmont, J. *The Chemistry of Inkjet Inks. Part II: Formulation and Materials for Inkjet Inks*; Magdassi, S., Ed.; World Scientific, 2009; pp 101−122. http://www.worldscientific.com/worldscibooks/10.1142/6869#t=toc, DOI: 10.1142/9789812818225_0006.